Proceedings of the 18th International Symposium on the Packaging and Transportation of Radioactive Materials
PATRAM 2016
September 18-23, 2016, Kobe, Japan

1060

The Estimation of potential Consequences from the Sabotage of Nuclear Material Transports

Marita Doehler
Gesellschaft für Anlagen- und Reaktorsicherheit (GRS) gGmbH, Cologne, Germany

Dr. Marcel Buchholz
Gesellschaft für Anlagen- und Reaktorsicherheit (GRS) gGmbH, Cologne, Germany

W. Koch
Department of Aerosol Technology, Fraunhofer ITEM, Hanover, Germany

H. Loedding
Department of Aerosol Technology, Fraunhofer ITEM, Hanover, Germany

A. Holzwarth
Fraunhofer EMI, Holzen, Germany

Abstract

A terrorist sabotage attack with explosives or explosively formed projectiles (EFP) against transport and storage casks could cause fragmentation of the (brittle) radioactive inventory and the formation and release of aerosol-borne radioactivity. For assessing the radiological consequences the characterization of the damage pattern of the cask and the source term, i.e. the release fraction defined as the fraction of the inventory released as (respirable) aerosols, needs to be determined. In order to quantify the release fraction and to observe the basic release mechanisms, a series of small scale experiments simulating sabotage attacks with explosives and EFPs was performed. In case of the experiments using explosives, various amounts of it were placed on steel panels, which were simulating the wall of the cask. In the “EFP-experiments” pre-manufactured flyer plates of 24 mm caliber were shot against a small-scale mock-up of a transport cask equipped with stainless-steel wall segments of variable thickness. Chemically doped quadratic ceramic plates, cylindrical concrete-targets and mock-ups of fuel elements filled with non-radioactive ceramic pellets were used as surrogates for brittle radioactive inventory inside of the casks. During the experiments the mass of two aerosol size fractions < 5 µm and < 10 µm, was measured by aerosol diagnostics. Temperature and pressure were recorded as additional input for numerical analysis and to model a potential outflow of gases out of casks. First results show, that release fractions determined during the experiments with explosives are in between 0.2 % and 2 % of the inventory surrogate compared to below 1 % in case of the experiments with EFPs. A dependence of the release fraction and the amount of explosives used, as well as on the thickness of the steel panel penetrated by the projectile was quantified, leading to specified correlations be-tween input energy and release

fraction. The results of the small scale experiments are supposed to serve as input data for the development of a predictive model to assess the aerosol release from explosive or EFP impact on casks during transport. In our contribution we will present the results and first analysis of the different experiments.

Introduction

Transported radioactive materials are frequently immobilized in brittle materials, e.g. cement/concrete, glass, ceramics, or are brittle materials by nature, such as fresh and spent fuel. A sabotage attack with explosives or an explosively formed projectile (EFP) on a transport and storage cask containing a radioactive inventory cause fragmentation of the (brittle) radioactive inventory and the formation and release of aerosol-borne radioactivity. International regulations on requirements for the transport of solid radioactive material are based among others on the potential release of aerosol-borne radioactivity under terrorist sabotage attacks.

There is an ongoing interest in quantifying the release of airborne radioactivity as a consequence of sabotage attacks on transport casks. So far, source terms for the release of aerosol-borne radioactivity have been extensively studied in small- and large-scale experiments in the context of HEDDs (high-energy density device) attacks on transport casks holding spent fuel [3-7]. Less is known about other possible scenarios, such as using explosively formed projectiles (EFPs). These devices can easily be assembled by terrorists and can be fired from a much larger standoff compared to HEDDs and still maintain their penetration capability.
The emission of respirable aerosols is determined by the size of the bullet hole, the aerosol formation upon interaction of the projectile with the brittle radioactive inventory inside the cask, and the aerosol transport processes from the inside through the bullet hole into the environment. Concerning the effects of explosives there are only few approaches how to estimate the amount of the respirable release of the mass of inert material caused by explosives. In those approaches, the influences of barriers in front of a target, like the wall of a cask, are neglected. For detonations in or contiguous to solid material, the respirable aerosol mass of inert material equal to the calculated TNT equivalent is assessed to be bounding [1]. Other experiments were performed in order to determine the robustness of different kinds of transport and storage casks regarding their resistance to explosives. Less information is available combining both the effects of the detonation on the cask and on the inventory. The emission of respirable aerosols is determined by the damage pattern of the cask, the aerosol formation upon the interaction of the shock wave with the brittle radioactive inventory inside the cask. For HEDDs the emission of respirable aerosols is determined by the size of the bullet hole, the aerosol formation upon interaction of the projectile with the brittle radioactive inventory inside the cask, and the aerosol transport processes from the inside through the bullet hole into the environment.

This paper describes the status of a joint effort of GRS and Fraunhofer aiming at measuring source terms in a small-scale mock-up system and to generate data-based knowledge for the development of a predictive release model.

Materials and methods

"Explosives"

A small-scale mock-up of a transport cask wall equipped with replaceable stainless steel wall segments of 20 mm thickness was used. Different amounts of explosive charges were directly mounted in front of the stainless steel wall segment. Chemically doped non-radioactive targets representing the brittle radioactive inventory were placed adjacent to the cask wall. The aerosol mass (m) is characterized by measuring aerosol concentrations inside the control volume confining the aerosol emitted from the targets (c). A sketch of the setup is shown in Fig. 1. Assuming well-mixed conditions in the control volume, the aerosol mass is determined from: $m=c \cdot V$ where V is the control volume.

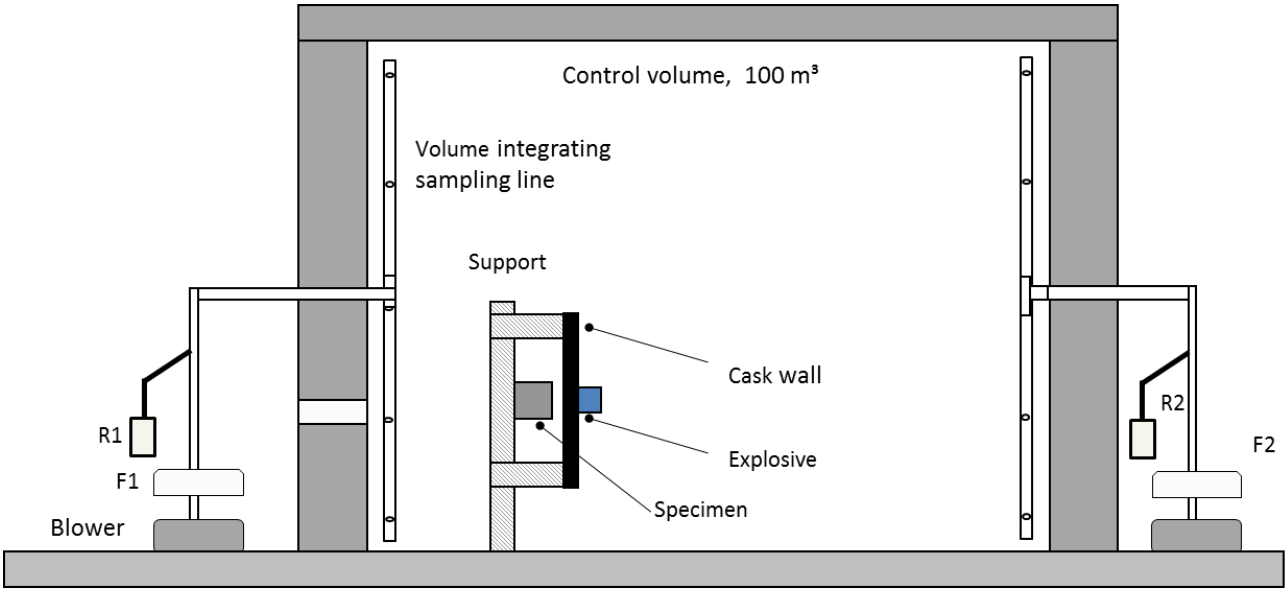

Figure 1 Experimental set-up for source term measurements

The concentration measurements were performed by collecting the relevant aerosol size fractions on filters and carrying out a chemical analysis of the tracer for the determination of the specific filter loading with the target material. The decrease of the aerosol concentration in the control volumes, caused among others by losses to the chamber walls during the sampling period (30 minutes), is taken into account by on-line optical concentration

recording.

Aerosol sampling and on-line monitoring were carried out using a combination of aerodynamic classification, filter sampling and aerosol photometry R1-R2 (Respicon TM, Helmut Hund GmbH, Wetzlar, Germany) operating at a flow rate of 3.1 L/min. Two of them are used in each compartment. In the large chamber, integrating sampling tubes sucking at 167 L/min from inlets at five heights above ground are used to perform a physical averaging of the vertical concentration distribution that may develop due to convection and particle settling. The two Respicons took a side-stream sample before the main flow was filtered (F1, F2). The sampling time was 1800 s for R1 and R2.

Cladded cement cylinders (length 10 cm, diameter 10 cm, ≈ 1900 g) were used as targets as well as mock-ups of fuel elements filled with non-radioactive ceramic pellets (5 by 5 arrays of 50-cm-long zircalloy fuel rods containing yttrium-stabilized zirconium oxide pellets). The cement targets were doped with rare-earth elements as chemical tracers.

Figure 2 Cement cylinder target setup “inside” (left) and fuel mock-up “inside” (right)

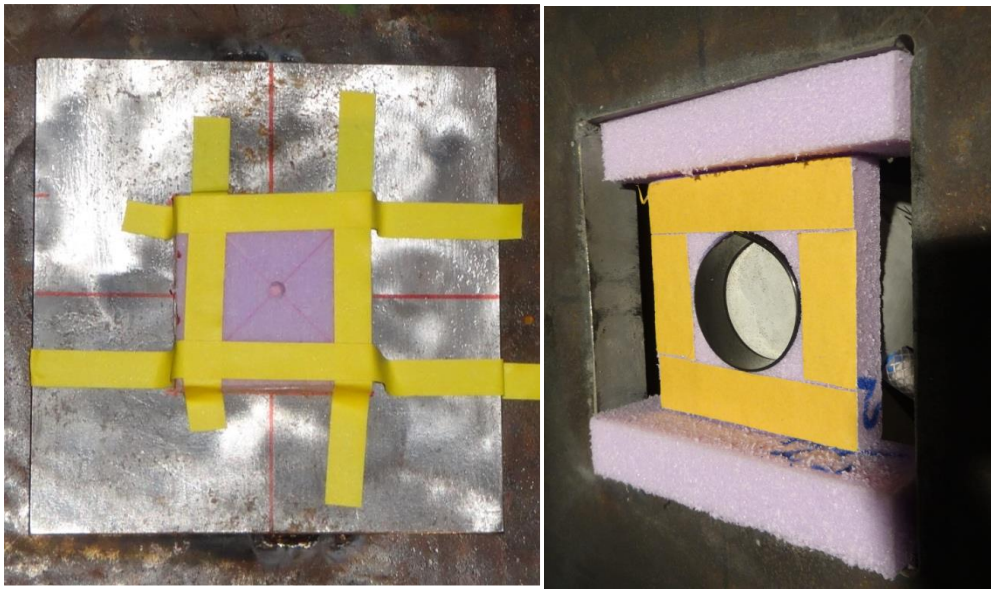

Figure 3 Stainless-steel plate with mounted explosives “outside” (left) that were used as a mock-up of a transport cask and mounting for explosives which is put on the target (right)

In total, ten experiments were performed. In six tests, three different amounts of explosives were used (50 g PETN, 120 g PETN and 200 g PETN). Furthermore, the distance between the cement target and the stainless steel plate was varied between 1 mm and 33 mm. Two tests were performed without any stainless-steel plate between the target and the explosive (30 g and 50 g PETN). Thereby, the explosive charge was directly mounted onto the cement cylinder. In another two tests mock-ups of fuel elements were used behind a steel plate.

“EFP”

Pre-manufactured flyer plates are impacted against a small scale mock-up of a transport cask equipped with stainless-steel wall segments of variable thickness. The aerosol mass (m_i) generated inside and released from the cask to the outside (m_o), respectively, is characterized by measuring aerosol concentrations inside the cask mock-up (c_i) and inside a control volume confining the aerosol emitted from the casks (c_o). Assuming well-mixed conditions in the two confinements, the masses are determined from: $m_{i,o}=c_{i,o}\cdot V_{i,o}$ where V_i , and V_o are the volumes of the cask mock-up and the outer control volume, respectively. The mock-up is equipped with replaceable stainless steel wall segments. Chemically doped non-radioactive targets representing the brittle radioactive inventory are placed adjacent to the cask wall. The concentration measurements inside and outside the cask were performed equivalent to the measurements during the experiments described before. Two Respicons are used in each compartment. In the large chamber, integrating sampling tubes sucking at 167 L/min from inlets at five heights above ground are used to perform a physical averaging

of the vertical concentration distribution that may develop due to convection and particle settling. The two Respicons took a side-stream sample before the main flow was filtered (F1, F2). The sampling time was 30 s for R3 and R4 and 1800 s for the monitors in the outer control volume.

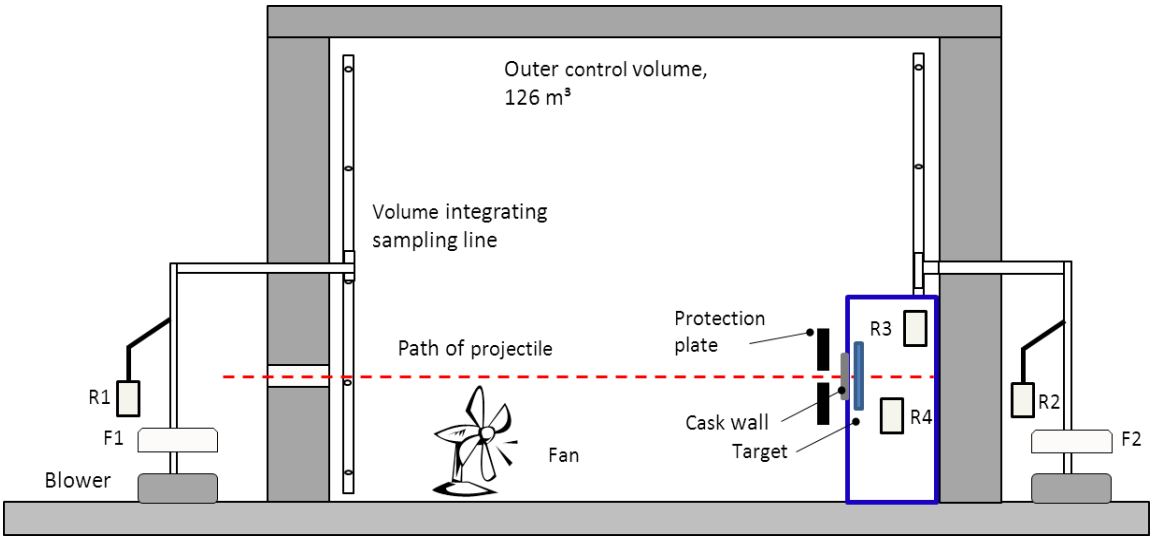

Figure 4 Experimental set-up for source term measurements

Three different types of targets were used (Fig. 5): quadratic 2-cm-thick ceramic plates (10x10 cm², 300 g, 20x20 cm², 1200 g), cladded cement cylinders (length 10 cm, diameter 10 cm, 1900 g), and again the mock-ups of fuel elements. The ceramic and cement targets were doped with rare-earth elements as chemical tracers. Dust released from damaged fuel rods was detected via yttrium analysis.

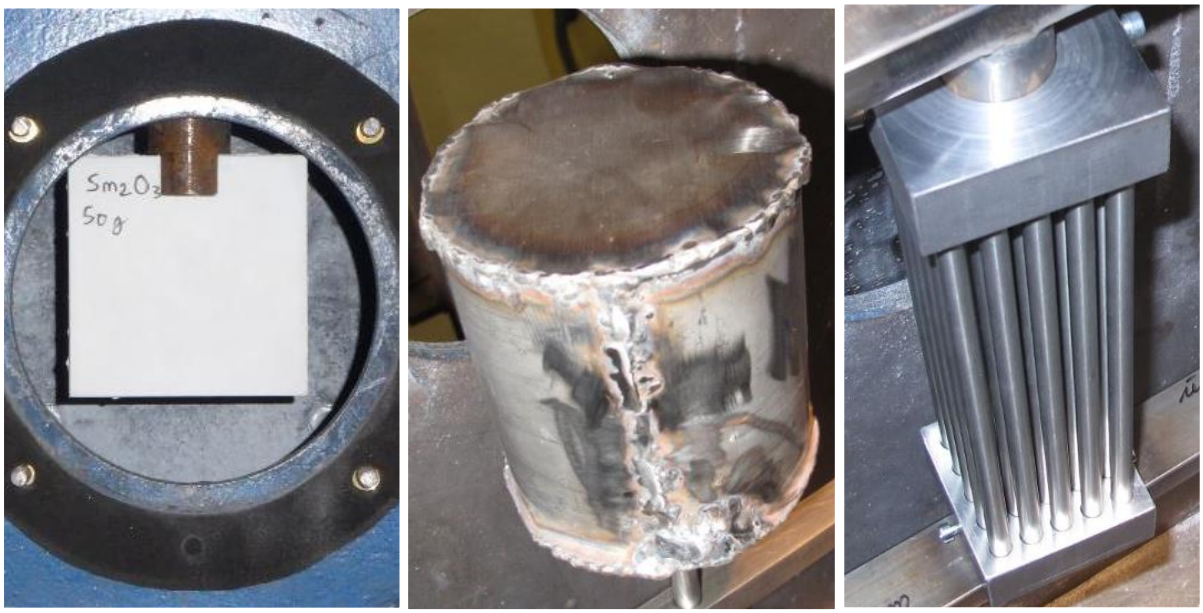

Figure 5 The three different target configurations used in the tests: ceramic plates

(left), cement cylinders (middle), fuel element mock-up (right).

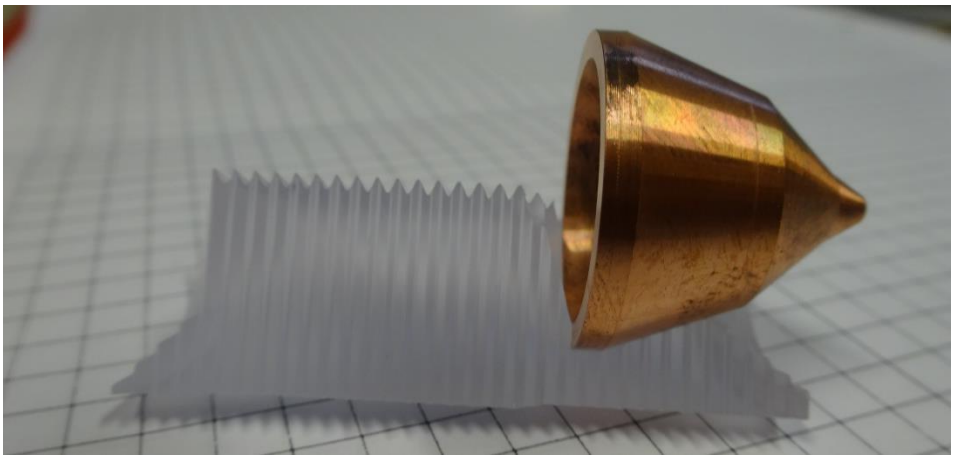

Figure 6 Bell-shaped flyer plate

Bell-shaped flyer plates (diameter 2.2 cm, mass 19 g) were embedded in a sabot (Fig. 6) and were accelerated in a powder gun to an intended velocity of 1.4 km/s resulting in a total steel penetration depth of the projectile of 25 mm, which is considerably larger than the maximum thickness of 10 mm of the wall plates selected during the tests. The actual impact velocity was measured directly in front of the cask mock-up. Temperature and pressure measurements were carried out inside the cask.

Results

“Explosives”

The damage of the cement cylinder caused by the explosives is shown in Fig. 7. Besides a small fraction of the target, the cement specimens underwent complete fragmentation characterized by fragments of different sizes, which is typical of fragmentation of brittle material [2]. The damage of the stainless steel plate caused by the explosives is shown in Fig. 8 for a small explosive charge and in Fig. 9 for a large explosive charge, respectively.

Figure 7 Photographs of the disintegrated cement cylinder target. (Test #2, 50 g explosive)

In both experiments with the small explosive charge, the transferred energy was not sufficient to create a hole inside the stainless-steel plate. The enlargement of the target-to-plate distance from 1 mm to 33 mm resulted in the separation of a stainless-steel disk as the deformation process of the steel plate was not stopped by any obstacle. For the small distance, this was not the case, as the energy used for deforming the plate was partly transferred on the fragmentation process of the cement cylinder.

Figure 8 Photographs of the damaged stainless-steel plate after interaction with the small explosive charge. Left: deformation for a distance of 1 mm between plate and target. Right: deformation for a distance of 33 mm between plate and target.

In both experiments with the large explosive charge, the transferred energy was sufficient to create a hole inside the stainless-steel plate and separate a fraction of the deformed material. The enlargement of the target-to-plate distance from 1 mm to 33 mm resulted in a more pronounced deformation pattern, in which a ring-like structure was separated.

Figure 9 Photographs of the damaged stainless-steel plate after interaction with the large explosive charge. Left: deformation for a distance of 1 mm between plate and target. Right: deformation for a distance of 33 mm between plate and target.

Quantitative results of the released fraction of respirable aerosol particles for four experiments with a stainless-steel plate mounted between the explosive and the target and for one test without such a plate are shown in Fig. 10. The generated fraction is defined as the mass of aerosol particles generated upon interaction with the explosives normalized to the target mass.

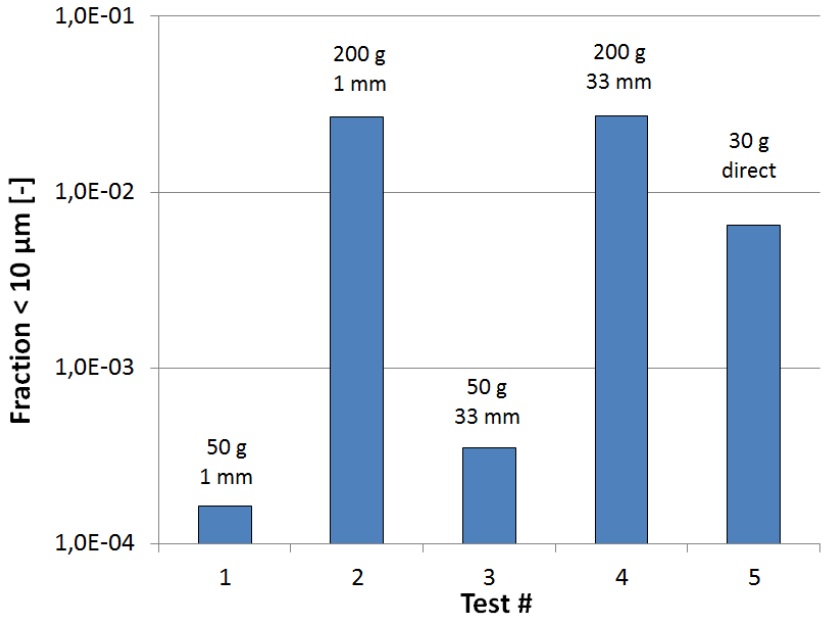

Figure 10 Generated dust upon interaction of explosive charges for 30 g, 50 g and 200 g PETN explosives and distances between the target and stainless-steel plate of 1 mm and 33 mm as well as without stainless steel plate.

In both tests with the 50 g explosive charge, respirable dust was generated inside the cask as a consequence of the deformation of the plate and the separation of a fraction of the plate. The energy was in both experiments not sufficient to create a hole inside the plate. Due to the intact cask wall, the respirable aerosol particles would remain inside the cask.

In both experiments with the 200 g explosive charge, the respirable fraction is approx. two orders of magnitude larger compared to the small charge. The dust would not stay inside the cask wall as the energy of the explosives was sufficient to create a hole inside the wall.

The influence of the target-to-wall distance is not yet completely clear. In the experiment with the small charge, the respirable fraction is enhanced by a factor of two for the larger distance as the deformed material was able to separate as a kind of projectile from the wall, accelerate, and interact with the target. In contrast, the generated fraction of aerosol particles for the large explosive charge is independent of this distance. Further studies have to be carried out to fully understand this relationship.

The tests, in which the explosive charge was directly mounted at the front of the target, shows that the respirable fraction of such a direct interaction is smaller by a factor of three than the amount of explosive charge equivalent to TNT. These findings are in good agreement with the estimates made in [2].

“EFP”

The damage caused by the interaction of the specimen with the EFP is shown in Fig. 11. The ceramic plates and the cement specimens underwent complete fragmentation characterized by fragments of all sizes, which is typical of fragmentation of brittle material [7]. The cladding of the cement cylinder did not change this qualitative picture.

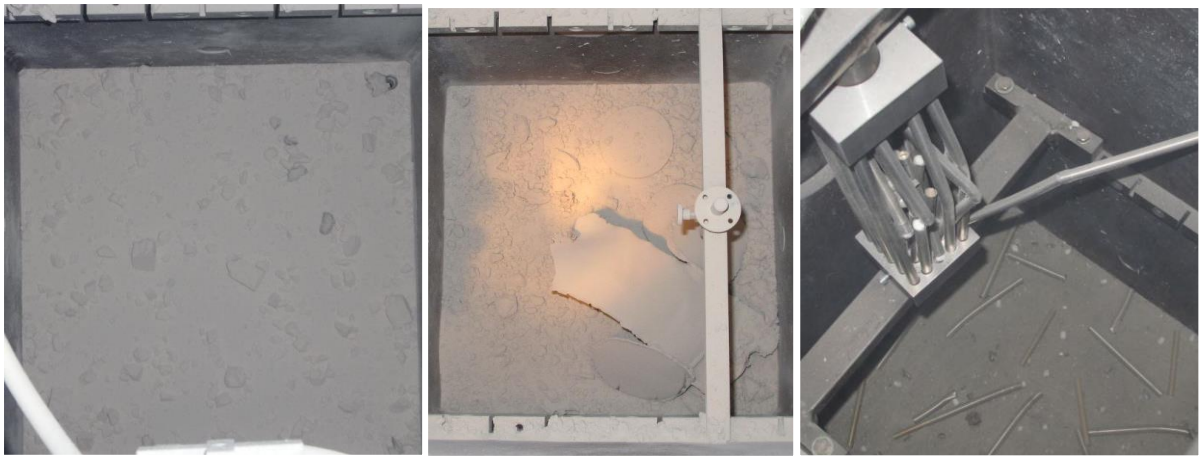

Figure 11 Photographs of the disintegrated specimens inside the box. Cement specimens underwent complete fragmentation characterized by fragments of all sizes (left & middle). Damage pattern of the fuel element mock-up (right).

Quantitative results of the six tests performed with the ceramic plates are shown in Fig. 12. The generated fraction is defined as the mass of aerosol particles generated upon interaction with the projectile normalized to the target mass. Similarly, the released fraction corresponds to the normalized aerosol mass ejected into the outer control volume. In all but the second test, the projectile penetrated centrally through the protection plate and created an inlet hole with a diameter of approx. 20 mm. In the second test, the projectile was misaligned and was slightly deformed by hitting the surface of the protection plate. A larger inlet hole was created and more dust was formed in this case due to a larger impact area of the projectile on the ceramic plate. The thickness of the wall plates has only little influence on dust generation as there is enough projectile energy remaining for complete fragmentation of the specimen. Impacting on the 20x20-plate leads to a reduction of mass-specific dust generation by a factor of 4.2 compared to the average values obtained from tests 3 to 4 due to the four-fold smaller ratio of impact area to the sample cross-sectional area.

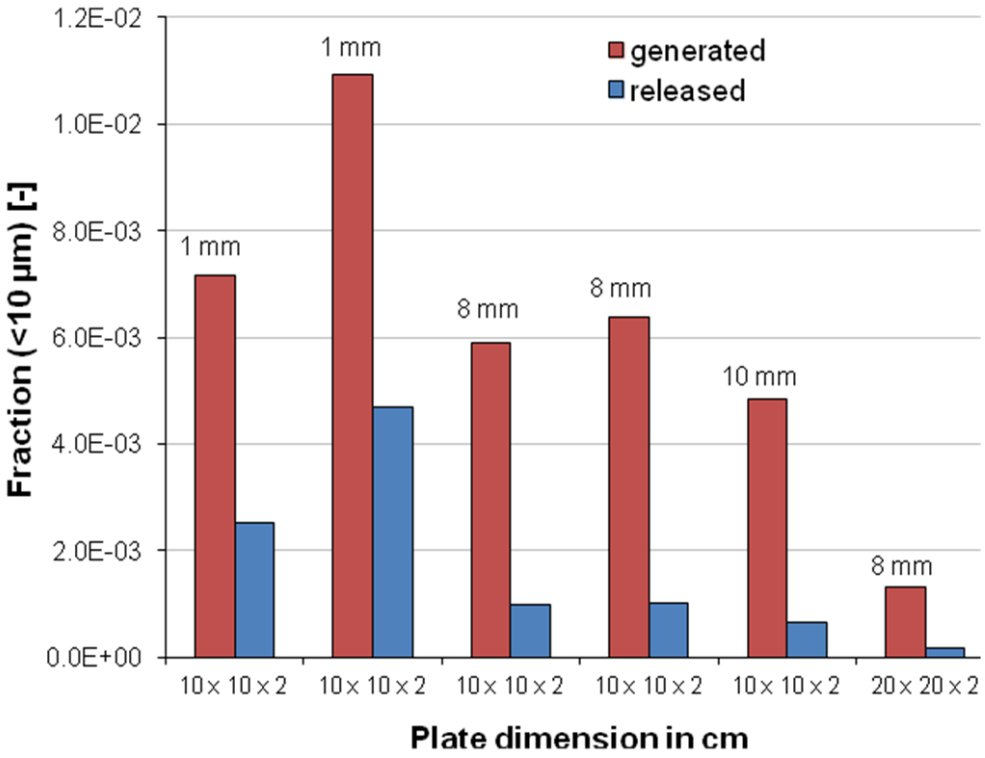

Figure 12 Generated and released dust upon interaction of an EFP with ceramic plates. Data index: thickness of the wall plate (length x height x width) of the cask mock-up.

For the 1 mm plate, around 40 % of the dust generated upon fragmentation was released into the atmosphere; for the 8 mm plates, this fraction was about 15%.

Acknowledgments

These works are funded by the BMUB under contract no. 3613R01605 and 3614R01620.

References

[1] DOE Handbook, Airborne Release Fractions/Rates and Respirable Fractions for Nonreactor Nuclear Facilities, Volume I – Analysis of Experimental Data

[2] F. Lange, F.,Martens, R., Nolte, O., Loedding, H., Koch, W., Hoermann, E. Testing of packages with LSA materials in very severe mechanical impact conditions with measurement of airborne release. Packaging, Transport, Storage & Security of Radioactive Materials, 2007, 18:59-71

[3] Molecke, M.A., J.E. Brockmann, D.A. Lucero, T.T. Borek, M.W. Gregson, R.E. Luna, M.C. Billone, T. Burtseva, W. Koch, O. Nolte, G. Pretzsch, F. Lange, W. Brücher, B. Autrusson and O. Loiseau, Spent Fuel Sabotage Test Program, Surrogate and Fission Product Aerosol Results, SAND2006-5556C, presented at the 47th Annual Meeting of the INMM Institute of Nuclear Materials Management, July 2006, Nashville, TN

[4] Brücher, W., Schmitz B., Schrödl E., Koch, W., Holzwart, A., Verbesserung der Quelltermermittlung für die Einwirkung panzerbrechender Waffen auf Transport- und Lagerbehälter mit abgebrannten Brennelementen, GRS, January 2012

[5] Sandoval, R.P., J.P. Weber, H.S. Levine, A.D. Romig, J.D. Johnson, R.E. Luna, G.J. Newton, B.A. Wong, R.W. Marshall, Jr., J.L. Alvarez, and F. Gelbard, An Assessment of the Safety of Spent Fuel Transportation in Urban Environs, SAND82-2365. Sandia National Laboratories. June 1983

[6] Lange, F., G, Pretzsch, J. Döhler, E. Hörmann, H. Busch, W. Koch. Experimental Determination for UO2 Release from a Spent Fuel Transport Cask after Shaped Charge Attack. Proc. INMM 35th Meeting, Naples, Florida. July 17-20, 1994.

[7] F. Lange, F.,Martens, R., Nolte, O., Lödding, H., Koch, W., Hörmann, E. Testing of packages with LSA materials in very severe mechanical impact conditions with measurement of airborne release. Packaging, Transport, Storage & Security of Radioactive Materials, 2007, 18:59-71